FUDMA Journal of Sciences (FJS)
ISSN online: 2616-1370
ISSN print: 2645 - 2944
Vol. 10 No. 12, June, 2026, pp 252 – 262
DOI: https://doi.org/10.33003/fjs-2026-1012-5665

Influence of Thermal Energy and Electronic Structure on the Refractive Index and Extinction Coefficient of $MAPbI_3$ Perovskite Solar Cell Materials

***Hassan Abdulsalam and Ibrahim Gana Geidam**

Department of Physics, Yobe State University, Damaturu, Yobe State, Nigeria.

*Corresponding authors' email: ahassanabdulsalam@gmail.com Phone No.: +234 8068061599

Received: 13th July 2026
Accepted: 15th July 2026
Published: 31st July 2026

ABSTRACT
The optical performance of perovskite solar cells depends strongly on the refractive index (n), extinction coefficient (k), temperature, and electronic structure of the absorber material. This study investigates the influence of thermal energy and bandgap variation on the optical constants of $MAPbI_3$ perovskite absorbers using temperature-dependent spectroscopic ellipsometry data obtained over 298.15–348.15 K and bandgap energies of 1.58–1.77 eV. Linear regression was used to determine the thermo-optic coefficients (dn/dT and dk/dT) and bandgap-sensitivity coefficients (dn/dE_g and dk/dE_g), while derivative spectroscopy identified wavelength regions with enhanced optical sensitivity. The results show that temperature causes only modest changes in optical dispersion and absorption, indicating good thermal stability. In contrast, bandgap variation significantly reduces the refractive index and shifts the absorption edge toward shorter wavelengths, demonstrating that electronic-structure modification has a stronger influence on optical behaviour than thermal effects. The highest sensitivities occur near the absorption edge, where interband transitions dominate. These findings highlight bandgap engineering as the primary strategy for tuning the optical properties of perovskite absorbers and provide useful guidance for the design of efficient and thermally stable perovskite solar cells.

Keywords: $MAPbI_3$ perovskites; Refractive index; Extinction coefficient; Thermo-optic coefficient; Bandgap engineering; Spectroscopic ellipsometry; Perovskite solar cells

INTRODUCTION

Hybrid organic–inorganic halide perovskites are among the most promising materials for next-generation photovoltaic and optoelectronic applications due to their strong optical absorption, tuneable bandgap, long carrier diffusion lengths, and solution-processable fabrication routes (Afre & Pugliese, 2024; Han *et al.*, 2025; Snaith, 2013). In particular, methylammonium lead iodide ($MAPbI_3$) has attracted significant attention owing to its direct bandgap (~1.5–1.6 eV), strong visible-light absorption, low exciton binding energy, and excellent charge transport properties(Snaith, 2013; Stranks & Snaith, 2015), making it a key model system for studying hybrid perovskite optoelectronics.

The optical response of $MAPbI_3$ is described by its complex refractive index, where the refractive index (n) governs light propagation and optical confinement, while the extinction coefficient (k) determines optical absorption (Fox, 2010; Pankove, 2012). These parameters critically influence reflection, transmission, absorption, and carrier generation in photovoltaic devices.

Perovskite optical properties are strongly temperature dependent due to lattice expansion, electron–phonon interactions, and bandgap renormalization (Kim *et al.*, 2021; Wright *et al.*, 2016). In operating conditions, temperatures can exceed 50–60 °C, affecting both n and k, particularly near the absorption edge where device performance is most sensitive (Ma *et al.*, 2025; Raja *et al.*, 2022). Understanding these effects is essential for reliable device design.

In addition to thermal effects, the bandgap plays a central role in determining optical behaviour. Bandgap variations, arising from compositional changes, structural disorder, and electron–phonon coupling, directly affect optical transitions and spectral response (Even *et al.*, 2013; Nie *et al.*, 2023; Wright *et al.*, 2016). Bandgap engineering is therefore a key strategy for optimizing perovskites in tandem solar cells and optoelectronic devices (Nie *et al.*, 2023).

Although many studies report perovskite optical properties, most focus on room-temperature conditions or treat thermal and electronic effects separately(Green *et al.*, 2014; Jeon *et al.*, 2015). Thus, the coupled influence of temperature and bandgap on $MAPbI_3$ optical constants remains insufficiently understood.

Therefore, this study investigates the combined influence of thermal energy and bandgap variation on the refractive index and extinction coefficient of $MAPbI_3$ using spectroscopic ellipsometry data. The work aims to clarify how lattice dynamics, electron–phonon interactions, and electronic structure collectively govern optical response, providing insights for improved perovskite solar-cell design.

Refractive Index and Extinction Coefficient

The optical response of a semiconductor material is described by its complex refractive index$\tilde{n}$,

$$\tilde{n} = n + ik \quad (1)$$

Where (n) is the refractive index and (k) is the extinction coefficient. The refractive index governs the propagation and phase velocity of electromagnetic waves within the material, whereas the extinction coefficient quantifies optical attenuation arising from photon absorption (Fox, 2010; Fujiwara, 2007).

The complex refractive index is related to the dielectric function through

$$\tilde{\varepsilon} = \varepsilon_1 + i\varepsilon_2 = (n + ik)^2 \quad (2)$$

From which $\varepsilon_1 = n^2 - k^2$ and $\varepsilon_2 = 2nk$ are obtained. Here, ε_1 and ε_2 represent the real and imaginary components of the dielectric response, respectively.

The extinction coefficient is related to the optical absorption coefficient by

$$\alpha = \frac{4\pi k}{\lambda} \quad (3)$$

Where λ is the wavelength of the incident radiation. Consequently, variations in (k) directly influence the absorption strength of the material, while changes in (n) determine optical dispersion and light propagation characteristics.

Thermal Energy Dependence of Optical Constants

Hybrid organic–inorganic perovskites exhibit strong temperature-dependent optical properties due to their soft crystal lattices, dynamic structural disorder, and pronounced electron–phonon interactions. The thermal energy associated with lattice vibrations is given by

$$E_{th} = k_B T \quad (4)$$

where k_B is Boltzmann's constant and (T) is the absolute temperature (Kittel, 2018).

As temperature increases, thermal expansion and enhanced lattice vibrations modify the local electronic environment, thereby altering both the refractive index and extinction coefficient (Ghosh, 1998; Peter & Cardona, 2010). Consequently, the optical constants become temperature-dependent functions:

$$n = n(\lambda, T) \quad (5)$$

And

$$k = k(\lambda, T) \quad (6)$$

For moderate temperature ranges, the temperature dependence of the optical constants can be approximated by (Saleh & Teich, 2013; Tropf *et al.*, 1998):

$$n(T) = n_0 + \beta_n T \quad (7)$$

And

$$k(T) = k_0 + \beta_k T \quad (8)$$

Where n_0 and k_0 represent the extrapolated optical constants at zero temperature, while β_n and β_k are the thermo-optic coefficients.

The thermo-optic coefficients are defined as (McLachlan & Meyer, 1987):

$$\beta_n = \frac{dn}{dT} \quad (9)$$

And

$$\beta_k = \frac{dk}{dT} \quad (10)$$

And quantify the sensitivity of optical dispersion and absorption to thermal perturbations. Positive values of β_n and β_k indicate an increase in the corresponding optical constant with temperature, whereas negative values indicate a decrease. These coefficients provide a quantitative measure of the thermal sensitivity of optical dispersion and absorption processes in perovskite materials (Ghosh, 1998; Handa *et al.*, 2020; Raja *et al.*, 2022).

Electronic Structure Dependence of Optical Constants

The optical properties of perovskite semiconductors originate from electronic transitions between occupied and unoccupied energy states. Consequently, the electronic bandgap (E_g) plays a central role in determining the refractive index, absorption coefficient, and overall optical response of the material (Even *et al.*, 2013).

The energy of an incident photon is given by

$$E = \frac{hc}{\lambda} \quad (11)$$

Where (h) is Planck's constant and (c) is the speed of light.

Near the absorption edge, the optical bandgap for a direct-transition semiconductor may be determined using the Tauc relation

$$(\alpha E)^2 = A\left(E - E_g^{opt}\right) \quad (12)$$

where (A) is a proportionality constant and E_g^{opt} is the optical bandgap (Tauc *et al.*, 1966).

The corresponding absorption-edge wavelength is related to the band gap by

$$\lambda_g = \frac{1240}{E_g} \quad (13)$$

Where E_g is expressed in electron volts (eV) and λ_g in nanometres (nm). An increase in bandgap energy shifts the absorption edge toward shorter wavelengths (blue shift), while a decrease in bandgap results in a red shift.

Since the optical response is governed by the electronic structure, the refractive index and extinction coefficient may be expressed as

$$n = n(\lambda, E_g) \quad (14)$$

And$k = k(\lambda, E_g)$ (15)

The sensitivity of optical constants to changes in bandgap is quantified by

$$\frac{dn}{dE_g} \quad (16)$$

And

$$\frac{dk}{dE_g} \quad (17)$$

These parameters describe the rate at which optical dispersion and absorption vary with electronic-structure modification and provide a direct measure of the influence of bandgap engineering on the optical response of perovskite materials.

To evaluate the effect of bandgap engineering on the optical response, the relative changes in the optical constants may be expressed as

$$\Delta n = n(E_g) - n(E_{g,ref}) \quad (18)$$

And$\Delta k = k(E_g) - k(E_{g,ref})$ (19)

Where $E_{g,ref}$ denotes a reference bandgap. These quantities provide a direct measure of how compositional tuning and electronic-structure modifications influence optical dispersion, absorption strength, and light–matter interactions within the perovskite lattice. Variations in the bandgap alter the density of electronic states, transition probabilities, and oscillator strengths, thereby affecting both the refractive index and extinction coefficient(Even *et al.*, 2013) (Minemoto & Murata, 2014; Raja *et al.*, 2022).

Derivative Spectroscopy

Derivative spectroscopy is an analytical technique used to enhance weak, overlapping, or poorly resolved spectral features that may not be readily visible in the original optical spectra. Rather than introducing new physical parameters, derivative spectroscopy utilizes the thermo-optic and bandgap-sensitivity coefficients defined in Sections 2.2 and 2.3 as wavelength-dependent spectral functions.

By analysing the spectral distributions of dn/dT, dk/dT, dn/dE_g, and dk/dE_g subtle changes associated with thermal perturbations and electronic-structure modifications can be identified with greater sensitivity than is possible from the original refractive-index and extinction-coefficient spectra. Peaks, extrema, and abrupt variations in these derivative spectra frequently correspond to critical points in the electronic band structure, enhanced electron–phonon coupling, or regions of strong interband optical transitions. Consequently, derivative spectroscopy provides valuable insight into the mechanisms governing optical dispersion, absorption behaviour, and light–matter interactions in perovskite absorbers.

In the present study, wavelength-dependent derivative spectra were employed to identify spectral regions exhibiting the highest sensitivity to temperature and bandgap variation, thereby revealing the dominant optical processes governing the thermo-optic and electronic responses of the material.

MATERIALS AND METHODS

Data Source and Description

The optical dataset employed in this study was obtained from the temperature-dependent optical characterization of triple-cation perovskite absorbers reported by Raja *et al*., (2022). The dataset consists of experimentally measured wavelength-dependent refractive index, n(λ,T), and extinction coefficient, k(λ,T), determined using spectroscopic ellipsometry. Measurements were conducted over a temperature range of 25–75 °C (298.15–348.15 K) and for absorber bandgap energies between 1.58 and 1.77 eV.

The dataset contains thirty independent optical spectra corresponding to six temperatures and five bandgap energies, providing comprehensive coverage of the near-band-edge spectral region where optical transitions are strongly influenced by thermal effects and electronic structure variations. The data were accessed and utilized under an American Chemical Society (ACS) RightsLink License Agreement (License No. 6264710405703), which permits academic reuse for research and publication purposes.

Data Pre-Processing

Prior to analysis, all temperature values were converted to Kelvin to ensure consistency in thermo-optic calculations. To independently evaluate thermal and electronic-structure effects, the dataset was divided into two subsets.

For the thermal analysis, the bandgap energy was fixed at 1.68 eV while the temperature was varied across 298.15, 308.15, 318.15, 328.15, 338.15, and 348.15 K. A wavelength range of approximately 751–1690 nm was selected for the refractive index analysis. This region corresponds to weak absorption conditions ($k \approx 0$), where the optical response is dominated by dispersion, thereby reducing non-linear effects and improving the reliability of linear regression for dn/dT and dk/dT.

For the electronic-structure analysis, the temperature was fixed at 318.15 K (45 °C) while the bandgap energy was varied from 1.58 to 1.77 eV. A wavelength range of approximately 826–1690 nm was also used for refractive index analysis within the weak absorption regime ($k \approx 0$). This ensures that the optical response is primarily governed by dispersion effects, enabling accurate extraction of dn/dEg and dk/dEg using linear regression.

This preprocessing approach isolates thermal and bandgap effects while ensuring statistically reliable linear fitting under quasi-transparent optical conditions.

Thermal Energy Analysis

The thermal energy analysis was performed by examining the evolution of the refractive index and extinction coefficient with temperature at a fixed bandgap energy of 1.68 eV. Spectral distributions of n (λ,T) and k(λ,T) were analysed over the temperature range of 298.15–348.15 K to evaluate the influence of thermal energy on optical dispersion and absorption behaviour.

Temperature-dependent variations in the magnitude and spectral position of the refractive-index and extinction-coefficient profiles were investigated to identify signatures of lattice expansion, enhanced electron–phonon scattering, and thermally induced modifications of interband transitions. Particular attention was given to shifts in the absorption-edge region and changes in optical dispersion, which provide insight into temperature-dependent light–matter interactions within the perovskite absorber.

To quantify the thermo-optic response, wavelength-dependent thermo-optic coefficients were obtained by fitting the optical constants to linear temperature-dependent models (Equations 6a and 6b).

Electronic Structure Analysis

The electronic-structure analysis was conducted at a fixed temperature of 318.15 K to isolate the influence of bandgap variation on the optical response. The study examined the evolution of therefractive index and extinction coefficient as the bandgap was varied from 1.58 to 1.77 eV, a range representative of compositional tuning strategies employed in tandem perovskite solar cells.

The analysis focused on the variation of optical dispersion, absorption onset, and refractive-index behaviour with increasing bandgap energy. The absorption-edge wavelength corresponding to each bandgap was estimated using Equation 10.

Additionally, the static refractive index and peak refractive-index positions were evaluated to assess how electronic-structure tuning influences optical polarization and transition probabilities. Relative changes in the optical constants were quantified using Equations 13a and 13b, where $E_{g,ref} = 1.58\ eV$ was selected as the reference bandgap. These parameters provide a direct measure of the influence of bandgap engineering on optical dispersion and absorption.

Derivative Spectroscopy Analysis

To enhance weak spectral features and quantify the sensitivity of the optical constants to thermal and electronic perturbations, derivative spectroscopy was employed. Derivative analysis provides increased sensitivity to subtle changes in optical behaviour that may not be readily observable in the original spectra.

Temperature Derivatives (dn/dT) and (dk/dT)

The temperature derivatives of the refractive index and extinction coefficient were determined using linear regression analysis at each wavelength. The slope of the temperature-dependent optical response was obtained using the Excel SLOPE function applied to the six-temperature dataset. The resulting thermo-optic coefficients were calculated as Equations 7a and 7b for every wavelength within the measured spectral range. The wavelength-dependent (dn/dT) and (dk/dT) spectra were subsequently analysed to identify spectral regions exhibiting strong thermo-optic sensitivity. Peaks and extrema in these spectra were interpreted as indicators of enhanced electron–phonon coupling and temperature-sensitive interband transitions.

Bandgap Derivatives (dn/dE_g) and (dk/dE_g)

The sensitivity of the optical constants to electronic-structure modifications was evaluated through the calculation of the bandgap derivatives Equations 12a and 12b using wavelength-dependent linear regression across the selected bandgap values at 318.15 K.

These derivative spectra quantify the response of optical dispersion and absorption to bandgap engineering and provide insight into the influence of compositional modifications on optical transition probabilities and oscillator strengths. Regions exhibiting large derivative magnitudes indicate wavelengths where the optical response is particularly sensitive to electronic-structurechanges, making them especially relevant for the design of wide-bandgap perovskite absorbers for tandem photovoltaic applications.

Data Visualization and Statistical Analysis

All data processing, regression analyses, derivative calculations, and graphical visualizations were performed

using Microsoft Excel. Wavelength-dependent spectra of the refractive index (n), extinction coefficient (k), and the corresponding sensitivity coefficients (dn/dT, dk/dT, dn/dE_g, and dk/dE_g) were generated to evaluate thermal and electronic-structure effects on the optical response. Linear regression was applied at each wavelength using the Excel SLOPE and INTERCEPT functions to determine the sensitivity coefficients and reference optical constants. The coefficient of determination (R^2) was calculated for all regressions to assess the validity of the linear approximation. The generally high R^2 values obtained across the investigated temperature and bandgap ranges confirmed the reliability of the regression-based approach for quantifying optical sensitivities.

RESULTS AND DISCUSSION

Regression Validity and Model Reliability

To evaluate the reliability of the linear regression approach used for extracting thermo-optic and bandgap-sensitivity parameters, the coefficient of determination (R^2) was calculated for all fitted models. Figure 1(a) presents the wavelength-dependent R^2 values for dn/dT and dk/dT, while Figure 1(b) shows the corresponding values for dn/dE_g and dk/dE_g.

Overall, the regressions exhibit high R^2 values across most of the investigated spectral range, indicating that the optical constants can be reasonably approximated as linear functions of temperature and bandgap energy within the selected operating ranges. The refractive-index regressions generally show stronger correlations than those of the extinction coefficient, suggesting that optical dispersion responds more uniformly to thermal and electronic perturbations than optical absorption. Localized reductions in R^2, particularly for dk/dEg, are most likely associated with the increased complexity of absorption processes near the band edge, where multiple electronic transitions and electron–phonon interactions contribute simultaneously to the optical response (Even *et al.*, 2013) (Wright *et al.*, 2016). Nevertheless, the predominance of high R^2 values confirms that the regression framework provides a robust basis for quantifying wavelength-dependent optical sensitivities.

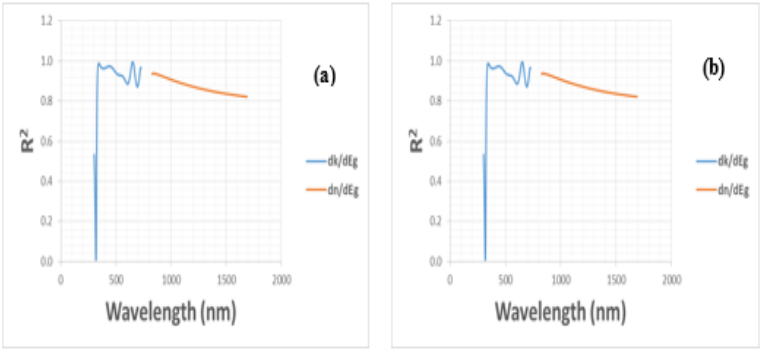

Figure 1: Wavelength-dependent coefficient of determination (R^2) for the regression models used to determine (a) thermo-optic coefficients (dn/dT and dk/dT) and (b) bandgap-sensitivity coefficients (dn/dEg and dk/dEg), demonstrating the reliability of the linear approximation across the investigated spectral range

Temperature-Dependent Optical Response

Temperature Dependence of the Refractive Index

Figure 2 shows the wavelength-dependent refractive-index spectra at a fixed bandgap energy of 1.68 eV for temperatures between 298.15 K and 348.15 K. The refractive index exhibits normal dispersion behaviour, increasing rapidly in the short-wavelength region before reaching a broad maximum near 450–700 nm and gradually decreasing toward longer wavelengths. A slight increase in refractive index is observed with increasing temperature across the entire spectral range. The temperature-induced variation is relatively small, indicating that the refractive index of the perovskite absorber is only moderately sensitive to thermal perturbations within the investigated temperature interval. This behaviour is consistent with temperature-induced modifications of lattice polarization and dielectric response arising from electron–phonon interactions in hybrid perovskites (Raja *et al.*, 2022; Wright *et al.*, 2016).

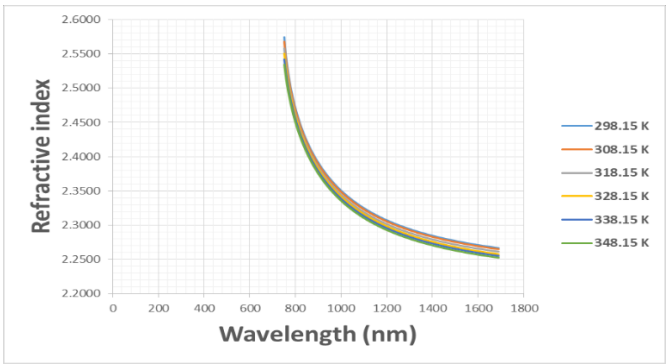

Figure 2: Wavelength-dependent refractive index (n) spectra of the perovskite absorber at a fixed bandgap energy of 1.68 eV for temperatures ranging from 298.15 K to 348.15 K, showing the influence of thermal energy on optical dispersion

Temperature Dependence of the Extinction Coefficient

Figure 3 presents the extinction-coefficient spectra at different temperatures for a fixed bandgap of 1.68 eV. The extinction coefficient reaches its maximum value in the near-band-edge region and decreases continuously with increasing wavelength. Increasing temperature produces only minor changes in the magnitude of the extinction coefficient, although slight spectral broadening is evident near the absorption edge. The weak temperature dependence suggests that thermal effects primarily influence the strength and broadening of optical transitions rather than significantly altering the overall absorption profile. Similar temperature-dependent broadening effects have previously been reported for hybrid perovskite absorbers and are commonly associated with enhanced phonon-assisted optical transitions at elevated temperatures (Raja *et al.*, 2022; Wright *et al.*, 2016).

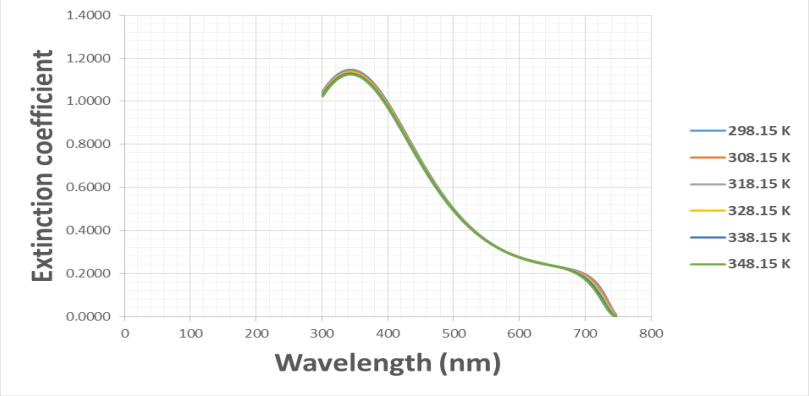

Figure 3: Wavelength-dependent extinction coefficient (k) spectra of the perovskite absorber at a fixed bandgap energy of 1.68 eV for temperatures ranging from 298.15 K to 348.15 K, illustrating the effect of temperature on optical absorption characteristics

Bandgap-Dependent Optical Response

Bandgap Dependence of the Refractive Index

Figure 4 illustrates the variation of the refractive index with wavelength for bandgap energies ranging from 1.58 to 1.77 eV at a fixed temperature of 318.15 K. The refractive index decreases systematically with increasing bandgap energy throughout the spectral range. The highest refractive-index values are observed for the smallest bandgap (1.58 eV), while the lowest values correspond to the widest bandgap (1.77 eV). This trend reflects the reduction in electronic polarizability associated with increasing bandgap energy and demonstrates the strong influence of electronic structure on optical dispersion. The observed inverse relationship between refractive index and bandgap energy is consistent with established semiconductor dispersion models and bandgap–refractive-index correlations reported in the literature. While initially quantified by the empirical Moss rule (Moss, 1950), this trend is fundamentally governed by the reduction in electronic polarizability and oscillator strength associated with widening the bandgap (Lamichhane, 2023). Recent studies have further unified these correlations using the Wemple–DiDomenico single-oscillator model (Lamichhane, 2023)and established specific refractive index–bandgap relationships tailored for perovskite structures (Khurgin, 2022; Lamichhane & Ravindra, 2022).

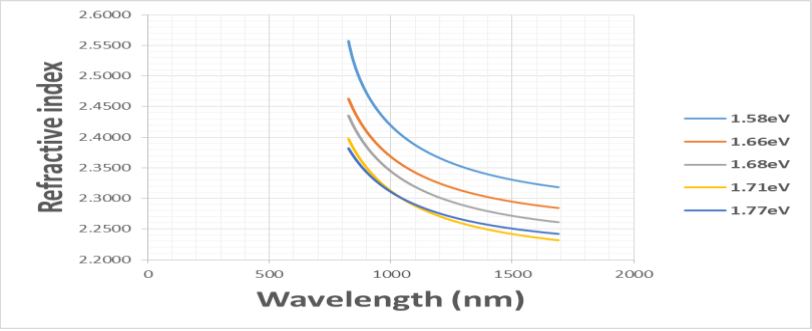

Figure 4: Wavelength-dependent refractive index (n) spectra of the perovskite absorber for bandgap energies between 1.58 and 1.77 eV at a fixed temperature of 318.15 K, demonstrating the influence of electronic structure on optical dispersion

Bandgap Dependence of the Extinction Coefficient

Figure 5 shows the extinction-coefficient spectra for different bandgap energies at 318.15 K. Increasing bandgap energy causes a noticeable shift of the absorption edge toward shorter wavelengths, indicating a clear blue shift. Simultaneously, the magnitude and spectral position of the absorption peak change significantly with bandgap energy. Compared with the temperature-dependent results, bandgap variation produces substantially larger modifications in the extinction coefficient, highlighting the dominant role of electronic structure in determining optical absorption characteristics. The observed blue shift occurs because wider-bandgapmaterials require higher photon energies to initiate interband electronic transitions, thereby shifting the absorption onset toward shorter wavelengths (Even *et al.*, 2013; Fox, 2010).

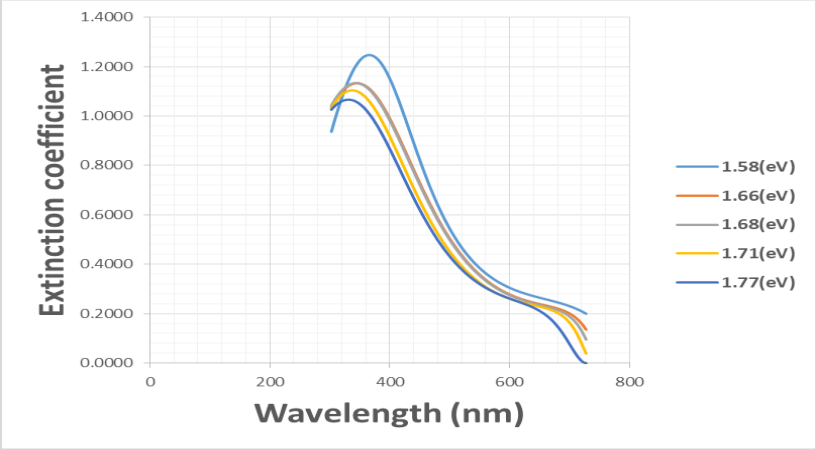

Figure 5: Wavelength-dependent extinction coefficient (k) spectra of the perovskite absorber for bandgap energies between 1.58 and 1.77 eV at a fixed temperature of 318.15 K, showing the effect of bandgap engineering on optical absorption and absorption-edge position

Comparative Analysis of Thermal and Electronic Structure Effects

Thermal Energy versus Electronic Structure Effects

A comparative examination of the temperature-dependent and bandgap-dependent optical responses reveals that electronic structure modifications exert a substantially greater influence on the optical constants than thermal energy variations. As shown in Figures 1 and 2, changes in temperature from 298.15 K to 348.15 K produce only modest variations in both the refractive index and extinction coefficient, with the spectra remaining closely grouped throughout the investigated wavelength range. In contrast, Figures 3 and 4 demonstrate significant separation of the optical spectra as the bandgap increases from 1.58 eV to 1.77 eV. The stronger dependence on bandgap energy indicates that compositional tuning and electronic-structure engineering are the primary mechanisms governing optical dispersion and absorption in the perovskite absorber. While thermal energy mainly affects the amplitude and broadening of optical transitions through lattice vibrations and electron–phonon interactions, bandgap variation directly modifies the energy levels involved in optical transitions, resulting in more pronounced changes in the optical response (Even *et al.*, 2013; Fox, 2010; Raja *et al*., 2022).

Spectral Evolution of the Optical Constants

The optical constants exhibit distinct spectral evolution in response to both temperature and bandgap variations. The refractive index spectra display normal dispersion behaviour characterized by an initial increase to a broad maximum in the visible region followed by a gradual decrease at longer wavelengths. The extinction coefficient exhibits strong absorption near the band edge and decreases progressively with increasing wavelength. Temperaturevariation primarily affects the magnitude and spectral broadening of these features, whereas bandgap variation significantly alters their spectral position and intensity. In particular, increasing bandgap energy causes a systematic blue shift of the absorption edge and a reduction in refractive index, reflecting the decreased electronic polarizability of wider-bandgap materials. These observations demonstrate that the evolution of the optical spectra is governed by the combined effects of lattice dynamics and electronic-structure modification, with the latter providing the dominant contribution to the observed optical behaviour(Even *et al.*, 2013; Wright *et al.*, 2016).

Thermo-Optic Coefficient Analysis

Wavelength Dependence of dn/dT and dk/dT

Figure 6 shows the wavelength dependence of the thermo-optic coefficients dn/dT and dk/dT obtained from regression analysis of the temperature-dependent optical spectra. These coefficients describe the rates at which the refractive index and extinction coefficient change with temperature and therefore provide a quantitative measure of the thermal sensitivity of optical dispersion and absorption.

The dn/dT spectrum exhibits relatively small values throughout the investigated wavelength range, indicating that the refractive index is only moderately affected by temperature variations between 298.15 K and 348.15 K. However, the coefficient is not constant across the spectrum, demonstrating that thermal effects influence optical dispersion differently at different photon energies. This behaviour reflects temperature-induced changes in dielectric polarization arising from lattice expansion and electron–phonon interactions(Peter & Cardona, 2010).

The dk/dT spectrum displays stronger wavelength dependence, particularly in the vicinity of the absorption edge. The enhanced sensitivity in this region indicates that optical absorption is more strongly affected by thermal perturbations than optical dispersion. Such behaviour is consistent with phonon-assisted optical transitions and temperature-induced broadening of electronic states, which become increasingly important near the onset of strong absorption (Raja *et al.*, 2022; Wright *et al.*, 2016). Overall, the results suggest that thermal effects primarily influence absorption processes while exerting a comparatively weaker effect on refractive-index dispersion.

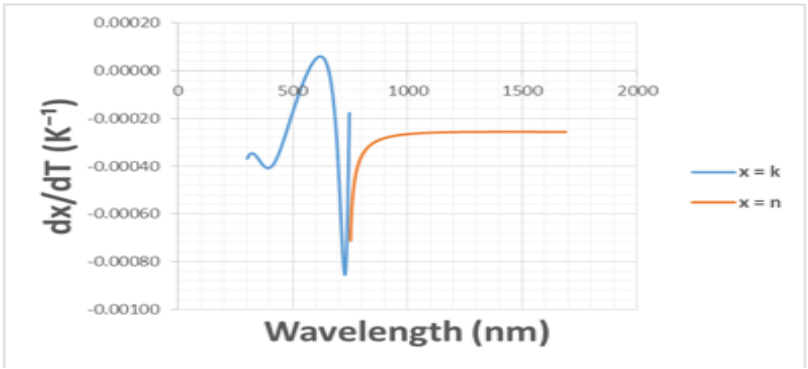

Figure 6: Wavelength-dependent thermo-optic coefficients (dn/dT and dk/dT) obtained from regression analysis of temperature-dependent optical spectra

Wavelength Dependence of $n_0$and k_0

Figure 7 presents the wavelength-dependent extrapolated optical constants n_0 and k_0 obtained from the intercepts of the temperature-dependent regression models. These parameters represent the intrinsic optical response of the material in the absence of thermal perturbations.

The n_0 spectrum exhibits the characteristic normal-dispersion behaviour observed in the measured refractive-index spectra, with relatively high values in the visible region followed by a gradual decrease at longer wavelengths. Likewise, the k_0 spectrum retains the typical absorption profile of the perovskite absorber, characterized by strong absorption near the band edge and progressively lower values toward longer wavelengths.

The similarity between the extrapolated and measured optical spectra indicates that temperature mainly modifies the magnitude and broadening of the optical response rather than its overall spectral shape. Consequently, the intrinsic optical behaviour remains predominantly governed by the electronic structure of the material, while thermal effects act as secondary perturbations superimposed on the underlying dispersion and absorption characteristics(Fox, 2010).

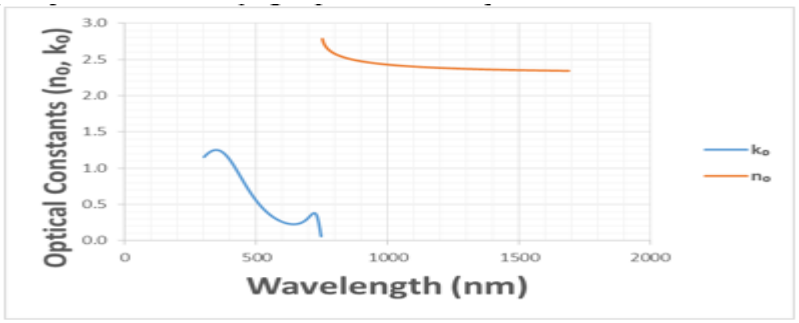

Figure 7: Wavelength-dependent extrapolated optical constants (n_0 andk_0) representing the intrinsic optical response at 0 K

Bandgap-Sensitivity Analysis

Wavelength Dependence of dn/dE_g and dk/dE_g

Figure 8 presents the wavelength-dependent bandgap-sensitivity coefficients dn/dE$_g$ and dk/dE$_g$. These parameters quantify the influence of electronic-structure modification on the optical constants and provide direct insight into the effects of bandgap engineering on optical behaviour. The dn/dEg spectrum is predominantly negative across most of the investigated wavelength range, indicating that the refractive index decreases with increasing bandgap energy. This behaviour is consistent with established semiconductor theories, which associate wider bandgaps with lower electronic polarizability and reduced refractive indices (Moss, 1950) (Fox, 2010). The magnitude of dn/dE$_g$ varies considerably with wavelength, demonstrating that the sensitivity of optical dispersion to bandgap tuning is strongly wavelength dependent.

Similarly, dk/dE$_g$ exhibits substantial spectral variation, with the largest magnitudes occurring near the absorption edge. The predominantly negative values indicate a reduction in optical absorption as the bandgap increases, reflecting the progressive blue shift of the absorption edge and the requirement for higher-energy photons to initiate interband transitions in wider-bandgap materials (Even *et al.*, 2013). The larger magnitudes observed for dk/dE$_g$ compared with dn/dE$_g$ further suggest that bandgap engineering has a stronger influence on absorption processes than on optical dispersion.

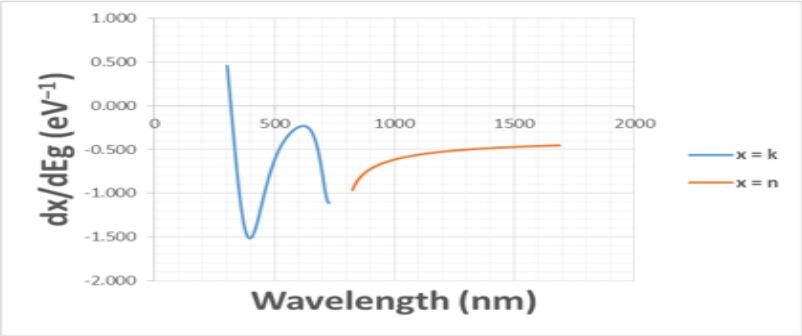

Figure 8: Wavelength-dependent bandgap-sensitivity coefficients (dn/dE_g and dk/dE_g) obtained from regression analysis of bandgap-dependent optical spectra

Wavelength Dependence of n_{ref} and k_{ref}

Figure 9 presents the wavelength-dependent reference optical constants, n_{ref} and k_{ref}, obtained from the intercepts of the bandgap-dependent regression models. These spectra represent the baseline optical response corresponding to the reference electronic structure utilized in the regression analysis. Both n_{ref} and k_{ref} retain the characteristic dispersion and absorption behaviour observed throughout the study, confirming that the overall spectral profiles remain governed by the intrinsic electronic structure of the perovskite absorber. However, a comparison of Figures 6–9 reveals that the magnitudes of dn/dE_g and dk/dE_g are generally greater than those of dn/dT and dk/dT, demonstrating that electronic structure modification induces substantially larger changes in the optical constants than thermal perturbations. This finding aligns with the earlier comparative analysis and reinforces that bandgap engineering is the dominant mechanism controlling optical dispersion and absorption in the investigated perovskite system. Ultimately, the strong sensitivity of both the refractive index and extinction coefficient to bandgap variation highlights the critical importance of compositional optimisation for tailoring the optical properties of high-efficiency perovskite and tandem solar cell architectures. (Even *et al.*, 2013; Raja *et al.*, 2022).

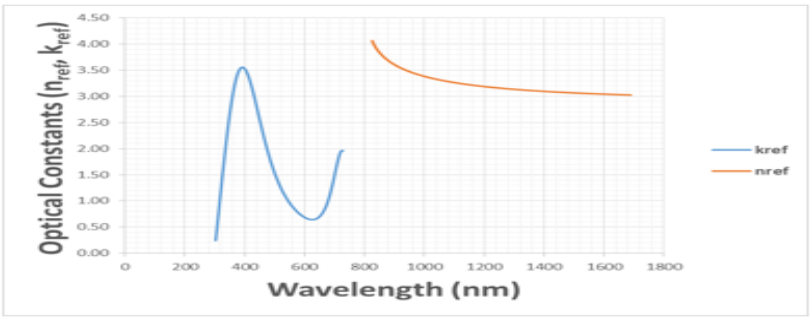

Figure 9: Wavelength-dependent reference optical constants (nref and kref) obtained from the intercepts of the bandgap-dependent regression models

Derivative Spectroscopy and Optical Sensitivity

Temperature Sensitivity of Optical Dispersion

The derivative spectrum dn/dT highlights spectral regions where refractive index is most responsive to temperature. Larger absolute values of dn/dT indicate wavelengths with strong thermo-optic effects, typically linked to electron–phonon coupling and temperature-dependent dielectric polarization. Similar behaviour has been reported in semiconductors and perovskites, where thermo-optic effects arise from lattice expansion and changes in electronic polarizability (Ghosh, 1998; Peter & Cardona, 2010). Overall, the small magnitude of dn/dT across most wavelengths confirms thermal stability, beneficial for photovoltaic operation under fluctuating conditions.

Temperature Sensitivity of Optical Absorption

The derivative spectrum dk/dT reveals that absorption is most temperature-sensitive near the band edge, where transitions are strongly influenced by lattice dynamics and phonon interactions. This behaviour reflects thermal broadening and phonon-assisted transitions, consistent with hybrid perovskite studies showing that temperature mainly redistributes transition probabilities rather than altering overall absorption (Raja *et al.*, 2022; Wright *et al.*, 2016). At longer wavelengths, the thermal impact diminishes.

Electronic Structure Sensitivity of Optical Dispersion

The derivative spectrum dn/dEg shows predominantly negative values, indicating that increasing bandgap energy reduces refractive index due to lower electronic polarizability. This inverse relationship aligns with semiconductor dispersion models(Fox, 2010; Moss, 1950). Compared with dn/dT, the magnitude of dn/dEg is much larger, confirming that bandgap engineering exerts stronger control over dispersion than thermal variation.

Electronic Structure Sensitivity of Optical Absorption

The derivative spectrum dk/dEg peaks near the absorption edge, where interband transitions dominate. Increasing bandgap energy shifts the edge to shorter wavelengths, producing significant changes in absorption strength. These results highlight that bandgap engineering has a far greater impact on absorption than thermal variation, making it the principal mechanism for tailoring optical properties (Even *et al.*, 2013; Minemoto & Murata, 2014).

Implications for Optical and Device Engineering of Perovskites

Thermal Stability and Optical Performance

Thermal perturbations produce modest changes in refractive index and absorption, with noticeable effects mainly near the band edge. This stability reduces temperature-induced efficiency losses, ensuring reliable operation under typical conditions. However, under extreme environments—such as high solar flux or elevated ambient temperatures—thermal broadening of states can still influence carrier dynamics and optical confinement. Effective **thermal management strategies** (e.g., encapsulation, heat dissipation layers) are therefore recommended to safeguard long-term stability (Ghosh, 1998; Peter & Cardona, 2010).

Bandgap Engineering and Optical Management

Bandgap engineering exerts a far stronger influence on optical behaviour than thermal variation. Adjusting bandgap energy through compositional tuning directly modifies dispersion, absorption strength, and the absorption-edge position. Derivative spectra identify wavelength regions most responsive to bandgap modification, enabling precise control of optical constants for enhanced light harvesting and spectral utilization. In practice, **optical management strategies** such as halide substitution, cation mixing, or alloying allow tailoring of bandgap values to match device requirements, improving optical confinement and maximizing photovoltaic efficiency (Even *et al.*, 2013; Minemoto & Murata, 2014).

Design Guidelines for High-Performance Devices

The combined insights from derivative spectroscopy and device engineering suggest clear design guidelines:

i. ***Maintain thermal stability*** by minimizing temperature-sensitive regions near the band edge.
ii. ***Exploit bandgap engineering*** to optimize dispersion and absorption for targeted spectral ranges.
iii. ***Integrate optical management techniques*** (anti-reflection coatings, textured interfaces, light-trapping layers) to maximize photon utilization. These strategies ensure that perovskite absorbers achieve both robustness and high efficiency in real-world applications.

Relevance to Tandem Perovskite Solar Cells

Wide-bandgap perovskites are essential as top absorbers in tandem architectures, where spectral matching between layers determines current balance and overall efficiency. Bandgap engineering enables the fine-tuning of the absorption edge and refractive index, ensuring optimal overlap with the spectral response of the bottom cell. Furthermore, derivative analysis highlights the spectral regions most sensitive to compositional modification, guiding material selection for tandem designs. Recent studies confirm that halide mixing or alloying can achieve the required blue shift of the absorption edge, establishing electronic structure engineering as the dominant strategy for tandem-cell optimization.(Green et al., 2025; NREL, 2022).

CONCLUSION

This study investigated the effects of thermal energy and electronic structure on the refractive index and extinction coefficient of MAPbI3 perovskite absorbers using temperature- and bandgap-dependent optical data. The results indicate that temperature induces only minor changes in optical dispersion and absorption, primarily driven by lattice vibrations and electron–phonon interactions. In contrast, bandgap variation significantly alters both optical constants, reducing the refractive index and shifting the absorption edge toward shorter wavelengths. Furthermore, the extracted thermo-optic and bandgap-sensitivity coefficients reveal a strong wavelength dependence, with the greatest sensitivities occurring near the absorption edge. Regression analysis confirmed the reliability of the linear sensitivity models across the investigated ranges. Overall, electronic-structure modification exerts a much stronger influence on optical behaviour than thermal energy. These findings demonstrate that bandgap engineering is the most effective approach for tailoring the optical properties of perovskite absorbers, providing valuable insights for the development of high-efficiency and thermally stable perovskite solar cells.

REFERENCES

Afre, R. A., & Pugliese, D. (2024). Perovskite solar cells: a review of the latest advances in materials, fabrication techniques, and stability enhancement strategies. Micromachines, 15(2), 192. https://doi.org/https://doi.org/10.3390/mi15020192

Even, J., Pedesseau, L., Jancu, J.-M., & Katan, C. (2013). Importance of spin–orbit coupling in hybrid organic/inorganic perovskites for photovoltaic applications. The Journal of Physical Chemistry Letters, 4(17), 2999-3005. https://doi.org/https://doi.org/10.1021/jz401532q

Fox, M. (2010). Optical properties of solids (2nd ed., Vol. 3). Oxford university press.

Fujiwara, H. (2007). Spectroscopic Ellipsometry: Principles and Applications. John Wiley & Sons. https://doi.org/https://doi.org/10.1002/9780470060193

Ghosh, G. (1998). Handbook of optical constants of solids: Handbook of thermo-optic coefficients of optical materials with applications. Academic Press.

Green, M. A., Dunlop, E. D., Yoshita, M., Kopidakis, N., Bothe, K., Siefer, G., Jiang, J. Y. (2025). Solar cell efficiency tables (version 66). Progress in Photovoltaics, 33(NREL/JA--5900-94273). https://doi.org/https://doi.org/10.1002/pip.3919

Green, M. A., Ho-Baillie, A., & Snaith, H. J. (2014). The emergence of perovskite solar cells. Nature photonics, 8(7), 506-514. https://doi.org/https://doi.org/10.1038/nphoton.2014.134

Han, J., Park, K., Tan, S., Vaynzof, Y., Xue, J., Diau, E. W.-G., Jeon, I. (2025). Perovskite solar cells. Nature Reviews Methods Primers, 5(1), 3. https://doi.org/https://doi.org/10.1038/s43586-024-00373-9

Handa, T., Yamada, T., Nagai, M., & Kanemitsu, Y. (2020). Phonon, thermal, and thermo-optical properties of halide perovskites. Physical Chemistry Chemical Physics, 22(45), 26069-26087. https://doi.org/https://doi.org/10.1039/D0CP04426A

Jeon, N. J., Noh, J. H., Yang, W. S., Kim, Y. C., Ryu, S., Seo, J., & Seok, S. I. (2015). Compositional engineering of perovskite materials for high-performance solar cells. Nature, 517(7535), 476-480. https://doi.org/https://doi.org/10.1038/nature14133

Khurgin, J. B. (2022). Expanding the photonic palette: exploring high index materials. Acs Photonics, 9(3), 743-751. https://doi.org/https://doi.org/10.1021/acsphotonics.1c01834

Kim, E.-B., Akhtar, M. S., Shin, H.-S., Ameen, S., & Nazeeruddin, M. K. (2021). A review on two-dimensional (2D) and 2D-3D multidimensional perovskite solar cells: Perovskites structures, stability, and photovoltaic performances. Journal of Photochemistry and Photobiology C: Photochemistry Reviews, 48, 100405. https://doi.org/https://doi.org/10.1016/j.jphotochemrev.2021.100405

Kittel, C. (2018). Kittel's Introduction to Solid State Physics, Global Edition. Wiley.

Lamichhane, A. (2023). Energy-gap-refractive index relations in semiconductors—using wemple–DiDomenico model to unify moss, ravindra, and herve–vandamme relationships. Solids, 4(4), 316-326. https://doi.org/https://doi.org/10.3390/solids4040020

Lamichhane, A., & Ravindra, N. M. (2022). Energy gap–refractive index considerations in perovskites. Emerging Materials Research, 11(4), 423-429. https://doi.org/https://doi.org/10.1680/jemmr.22.00053

Afre, R. A., & Pugliese, D. (2024). Perovskite solar cells: a review of the latest advances in materials, fabrication techniques, and stability enhancement strategies. Micromachines, 15(2), 192. https://doi.org/https://doi.org/10.3390/mi15020192

Even, J., Pedesseau, L., Jancu, J.-M., & Katan, C. (2013). Importance of spin–orbit coupling in hybrid organic/inorganic perovskites for photovoltaic applications. The Journal of Physical Chemistry Letters, 4(17), 2999-3005. https://doi.org/https://doi.org/10.1021/jz401532q

Fox, M. (2010). Optical properties of solids (2nd ed., Vol. 3). Oxford university press.

Fujiwara, H. (2007). Spectroscopic Ellipsometry: Principles and Applications. John Wiley & Sons. https://doi.org/https://doi.org/10.1002/9780470060193

Ghosh, G. (1998). Handbook of optical constants of solids: Handbook of thermo-optic coefficients of optical materials with applications. Academic Press.

Green, M. A., Dunlop, E. D., Yoshita, M., Kopidakis, N., Bothe, K., Siefer, G., Jiang, J. Y. (2025). Solar cell efficiency tables (version 66). Progress in Photovoltaics, 33(NREL/JA--5900-94273). https://doi.org/https://doi.org/10.1002/pip.3919

Green, M. A., Ho-Baillie, A., & Snaith, H. J. (2014). The emergence of perovskite solar cells. Nature photonics, 8(7), 506-514. https://doi.org/https://doi.org/10.1038/nphoton.2014.134

Han, J., Park, K., Tan, S., Vaynzof, Y., Xue, J., Diau, E. W.-G., Jeon, I. (2025). Perovskite solar cells. Nature Reviews Methods Primers, 5(1), 3. https://doi.org/https://doi.org/10.1038/s43586-024-00373-9

Handa, T., Yamada, T., Nagai, M., & Kanemitsu, Y. (2020). Phonon, thermal, and thermo-optical properties of halide perovskites. Physical Chemistry Chemical Physics, 22(45), 26069-26087. https://doi.org/https://doi.org/10.1039/D0CP04426A

Jeon, N. J., Noh, J. H., Yang, W. S., Kim, Y. C., Ryu, S., Seo, J., & Seok, S. I. (2015). Compositional engineering of perovskite materials for high-performance solar cells. Nature, 517(7535), 476-480. https://doi.org/https://doi.org/10.1038/nature14133

Khurgin, J. B. (2022). Expanding the photonic palette: exploring high index materials. Acs Photonics, 9(3), 743-751. https://doi.org/https://doi.org/10.1021/acsphotonics.1c01834

Kim, E.-B., Akhtar, M. S., Shin, H.-S., Ameen, S., & Nazeeruddin, M. K. (2021). A review on two-dimensional (2D) and 2D-3D multidimensional perovskite solar cells: Perovskites structures, stability, and photovoltaic performances. Journal of Photochemistry and Photobiology C: Photochemistry Reviews, 48, 100405. https://doi.org/https://doi.org/10.1016/j.jphotochemrev.2021.100405

Kittel, C. (2018). Kittel's Introduction to Solid State Physics, Global Edition. Wiley.

Lamichhane, A. (2023). Energy-gap-refractive index relations in semiconductors—using wemple–DiDomenico model to unify moss, ravindra, and herve–vandamme relationships. Solids, 4(4), 316-326. https://doi.org/https://doi.org/10.3390/solids4040020

Lamichhane, A., & Ravindra, N. M. (2022). Energy gap–refractive index considerations in perovskites. Emerging Materials Research, 11(4), 423-429. https://doi.org/https://doi.org/10.1680/jemmr.22.00053

Ma, L., Xu, X., Cui, C., Li, T., Lou, S., Scott, P. J., Zeng, W. (2025). A review of measurement and characterization of film layers of perovskite solar cells by spectroscopic ellipsometry. Nanomaterials, 15(4), 282. https://doi.org/https://doi.org/10.3390/nano15040282

McLachlan, A. D., & Meyer, F. P. (1987). Temperature dependence of the extinction coefficient of fused silica for CO2 laser wavelengths. Applied Optics, 26(9), 1728-1731. https://doi.org/https://doi.org/10.1364/AO.26.001728

Minemoto, T., & Murata, M. (2014). Device modeling of perovskite solar cells based on structural similarity with thin film inorganic semiconductor solar cells. Journal of applied physics, 116(5). https://doi.org/https://doi.org/10.1063/1.4891982

Moss, T. (1950). A relationship between the refractive index and the infra-red threshold of sensitivity for photoconductors. Proceedings of the Physical Society. Section B, 63(3), 167-176. https://doi.org/https://doi.org/10.1088/0370-1301/63/3/302

Nie, T., Fang, Z., Ren, X., Duan, Y., & Liu, S. (2023). Recent advances in wide-bandgap organic–inorganic halide perovskite solar cells and tandem application. Nano-Micro Letters, 15(1), 70. https://doi.org/https://doi.org/10.1007/s40820-023-01040-6

NREL. (2022). Best Research-Cell Efficiency Chart. https://www.nrel.gov/pv/cell-efficiency.html

Pankove, J. I. (2012). Optical processes in semiconductors. Courier Corporation. https://doi.org/https://doi.org/10.1149/1.2404256

Peter, Y., & Cardona, M. (2010). Fundamentals of semiconductors: physics and materials properties. Springer Science & Business Media. https://doi.org/https://doi.org/10.1007/978-3-642-00710-1

Raja, W., Allen, T. G., Said, A. A., Alharbi, O., Aydin, E., De Bastiani, M., & De Wolf, S. (2022). Temperature-dependent optical modeling of perovskite solar cells. The Journal of Physical Chemistry C, 126(33), 14366-14374. https://doi.org/https://doi.org/10.1021/acs.jpcc.2c04768

Saleh, B. E. A., & Teich, M. C. (2013). Fundamentals of Photonics. Wiley.

Snaith, H. J. (2013). Perovskites: the emergence of a new era for low-cost, high-efficiency solar cells. The Journal of Physical Chemistry Letters, 4(21), 3623-3630. https://doi.org/https://doi.org/10.1021/jz4020162

Stranks, S. D., & Snaith, H. J. (2015). Metal-halide perovskites for photovoltaic and light-emitting devices. Nature nanotechnology, 10(5), 391-402. https://doi.org/https://doi.org/10.1038/nnano.2015.90

Tauc, J., Grigorovici, R., & Vancu, A. (1966). Optical properties and electronic structure of amorphous germanium. physica status solidi (b), 15(2), 627-637. https://doi.org/https://doi.org/10.1002/pssb.19660150224

Tropf, W. J., Thomas, M. E., & Linevsky, M. J. (1998). Infrared refractive indices and thermo-optic coefficients for several materials. Optical Diagnostic Methods for Inorganic Transmissive Materials,

Wright, A. D., Verdi, C., Milot, R. L., Eperon, G. E., Pérez-Osorio, M. A., Snaith, H. J.,…Herz, L. M. (2016). Electron–phonon coupling in hybrid lead halide perovskites. Nature communications, 7(1), 11755. https://doi.org/https://doi.org/10.1038/ncomms11755